Effects of Attached Masses on Free Vibration of Rigid Point Supported Rectangular Plates

R. K. Singal*
Canadian Space Agency, Ottawa, K2H 8S2 Canada
and
D. J. Gorman†
University of Ottawa, Ottawa, K1N 6N5 Canada

I. Introduction

THE problem of predicting free vibration frequencies and mode shapes for thin elastic plates resting on discrete point supports has been fairly well resolved in recent years. Excellent agreement in the results obtained by various researchers using different analytical techniques is discussed in Ref. 1 and in references contained therein.

More recently, the present authors have addressed the even more challenging problem of obtaining accurate free vibration analysis of rectangular plates resting on what has been referred to as rigid point supports. This terminology implies that the support at a point is such that not only is lateral movement of the plate forbidden, as is the case with discrete point supports, but slope taken in any direction from the point is also forbidden. This is the type of support that is normally encountered when the plate is fixed at a point by a screw-type fastener, or by a local weld spot. A strong interest in the behavior of plates with this latter type of support has arisen in connection with the design of electronic circuit boards, solar collector panels, etc.

In Ref. 2, the authors have described in detail an analytical and experimental approach to resolve this problem. The analysis was based on the superposition method as developed earlier by the second author.[1] Rigid point supports were modeled mathematically by utilizing an appropriate cluster of four local discrete point supports. An extensive experimental test program was carried out in support of the analysis. Excellent agreement between theory and experiment was obtained for a wide range of rigid point support distributions.

The principal objective of the work reported here is to describe the results of a natural extension of the previously mentioned research program in which, in addition to rigid point supports, the vibration problem was complicated by the presence of local masses attached to the plate surface. It will be appreciated that in many practical problems, such as the design of electronic circuit boards, there will, in fact, be local masses attached to the boards at various points throughout the lateral surface. The same situation may be encountered in solar collector panels. The object of this Note is to present the experimental and theoretical findings obtained in connection with this latter family of problems.

II. Analytical Procedure

The method of analysis is essentially an extension of that described in Ref. 2. For this reason, only a very brief description of the analytical procedure is given here for the sake of completeness. Emphasis will be placed on the modifications necessary in order to take into account the effects of the added masses.

The overall solution to any problem is obtained by superimposing Lévy-type solutions to a set of forced vibration problems, as depicted schematically in Fig. 1 and described in Ref. 2. Each of the first four building blocks in the figure is driven along one edge by a distributed harmonic bending moment or rotation. These driving moments are expanded in a Fourier cosine series. All edges are free of vertical edge reaction and all nondriven edges are given slip-shear support, i.e., vertical edge reaction is zero and slope taken normal to the edge is everywhere zero.

All building blocks (Lévy-type solutions) beyond the first four are driven by an appropriately located concentrated harmonic force. Four such building blocks are required for each location of rigid point support and one is required to handle the effect of each attached mass. In the earlier problem, a solution was obtained by superimposing all of the required building blocks and constraining the Fourier coefficients appearing along the boundaries, and the amplitudes of the concentrated harmonic forces, so as to satisfy the condition of zero net moment along the plate edges and zero net lateral displacement at the individual point supports. By a judicious clustering of the four individual point supports, at each location of rigid point support, the required support conditions were achieved. The only additional theoretical considerations pertaining to the present work relate to the existence of concentrated inertia forces arising because of the presence of attached masses. The amplitude of the inertia force exerted on the plate by an attached mass M is written as

$$P = M\omega^2 a\, W(u, v) \tag{1}$$

where u and v are the dimensionless coordinates (distances divided by plate edge lengths a and b, respectively) of the attached mass, W equals the amplitude of the plate lateral vibration divided by a, and ω equals circular frequency of vibration.

The free vibration eigenvalue is defined as λ^2, where $\lambda^2 = \omega a^2 \sqrt{\rho/D}$, ρ is the mass per unit area of the plate and D is its flexural rigidity. The concentrated driving force may therefore be written as

$$P^* = -2\phi^4 M_r \lambda^4 W(u, v) \tag{2}$$

where ϕ is the plate aspect ratio b/a and M_r equals the ratio of the attached mass to the mass of the plate.

Let us now suppose we have numerous building blocks involving concentrated driving forces. Then total displacement at the specifc point (u, v) as just discussed will be written as $P_1^* W_1(u, v) + P_2^* W_2(u, v) + \ldots +$ displacement at (u, v) due to the first four building blocks.

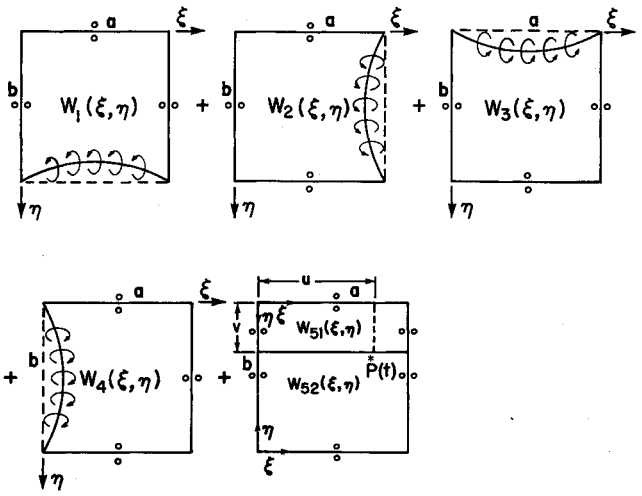

Fig. 1 Four building blocks utilized in analysis of completely free rectangular plate plus building block with harmonic driving force $P^*(u, v)$.

Received Jan. 22, 1991; revision received May 18, 1991; accepted for publication May 30, 1991.

*Research Scientist, Directorate of Space Mechanics.
†Professor, Department of Mechanical Engineering.

Table 1 Measured and computed frequencies (Hz) for plates A and B with single attached mass at center of plate (experimental values in parentheses)

	Attached mass, g													
	0		50		100		150		200		250		300	
	A	B	A	B	A	B	A	B	A	B	A	B	A	B
0.05	54.9 (55.4)	65.0 (65.6)	47.4 (48.4)	56.8 (57.7)	42.1 (43.1)	50.3 (51.6)	38.1 (39.2)	45.6 (47.0)	35.1 (36.2)	41.9 (43.1)	32.7 (33.9)	38.9 (40.3)	30.7 (31.9)	36.5 (37.9)
0.10	75.6 (74.4)	81.0 (81.6)	63.4 (63.7)	70.8 (71.2)	55.1 (55.8)	61.8 (62.8)	49.3 (50.1)	55.4 (56.6)	45.0 (45.9)	50.5 (51.8)	41.6 (42.5)	46.7 (48.0)	38.8 (39.8)	43.6 (44.9)
0.15	102.4 (100.8)	104.2 (103.0)	83.1 (84.6)	89.2 (88.7)	70.5 (72.7)	76.0 (76.8)	62.2 (64.5)	67.2 (68.4)	56.2 (58.7)	60.8 (62.0)	51.6 (54.0)	55.8 (57.1)	48.0 (50.4)	51.9 (53.1)
0.20	138.1 (137.6)	136.7 (134.3)	108.9 (111.7)	113.4 (114.0)	90.0 (93.5)	94.2 (96.8)	78.3 (81.9)	82.0 (84.9)	70.1 (73.4)	73.5 (76.4)	64.0 (67.2)	67.1 (69.9)	59.3 (62.3)	62.1 (64.6)
0.25	127.6 (126.8)	127.6 (126.8)	125.2 (125.1)	125.2 (125.1)	113.8 (117.4)	113.8 (117.4)	99.2 (103.8)	99.2 (103.8)	88.4 (93.2)	88.4 (93.2)	80.4 (84.6)	80.4 (84.6)	74.2 (78.6)	74.2 (78.6)
0.30	91.0 (88.8)	92.1 (89.8)	90.9 (88.8)	92.0 (88.4)	90.8 (88.8)	91.8 (88.7)	90.6 (88.8)	91.4 (88.4)	90.5 (88.5)	90.8 (88.1)	90.0 (88.5)	89.2 (87.6)	88.9 (88.1)	85.9 (86.4)
0.35	67.0 (66.2)	68.9 (68.6)	67.0 (66.1)	68.9 (68.6)	67.0 (66.1)	68.8 (68.6)	67.0 (66.0)	68.8 (68.5)	67.0 (66.1)	68.7 (68.5)	67.0 (66.1)	68.7 (68.5)	67.0 (66.1)	68.7 (68.4)
0.40	50.5 (48.2)	53.4 (55.4)	50.5 (48.2)	53.4 (55.3)	50.5 (48.2)	53.4 (55.3)	50.5 (48.3)	53.4 (55.2)	50.5 (48.3)	53.4 (55.2)	50.5 (48.3)	53.4 (55.2)	50.5 (48.1)	53.3 (55.2)

In fact, if we require zero displacement at the point (u, v), as is the case for all discrete support points as discussed in Ref. 2, one of the rows in the lower portion of the eigenvalue matrix will enforce the condition that total displacement as expressed earlier will equal zero. Let us suppose, on the other hand, that at a point (u, v) on the plate we have an attached mass. Let us refer to this as the n'th point with dimensionless driving force amplitude P_n^*. It is now easy to modify the relevant previously mentioned row of the eigenvalue matrix to satisfy Eq. (2) instead of the zero net deflection condition. We simply go along this row until we come to the element immediately below P_n^*. To this element we add the quantity $1/(2\,\phi^4 M_r \lambda^4)$.

In summary, we should generate the eigenvalue matrix as though all concentrated driving forces were utilized to eliminate the net plate displacement at their point of application, as described in Ref. 2. Finally, we should return only to the elements of the matrix as described earlier, which are associated with inertia forces due to attached masses and make the appropriate postmodifications. Such postmodifications are easily programmed into the computer routine. With the eigenvalue matrix established, the eigenvalues are obtained in the usual manner by searching for those values of λ^2 that cause the determinant of the eigenvalue matrix to vanish.

III. Presentation of Theoretical and Experimental Results

A. Description of Experimental Test Specimens

All experimental tests were conducted on aluminum plates of 10.0 × 15.0 in. (25.4 × 38.1 cm) × 0.0625 in. (1.59 mm) thick. Two plate families, A and B, each with four symmetrically distributed rigid point supports, were employed. In plate A tests, four rigid point supports were symmetrically located on the plate diagonals, as indicated in Fig. 2a. The dimensionless coordinates of these supports are designated by U, the distance in the coordinate direction divided by the edge length running parallel to the direction. The parameter U was allowed to take on values from 0.05 to 0.40 in intervals of 0.05. In plate B tests, experiments were conducted in a fashion similar to those described for plate A except that support points were located along the two straight lines running parallel to the long edges and one quarter of the way in, as indicated in Fig. 2b.

For each of the rigid support point configurations as described earlier, tests were conducted for three different mass configurations. In the first configuration, a single mass was located at the center of the plate. In the second configuration,

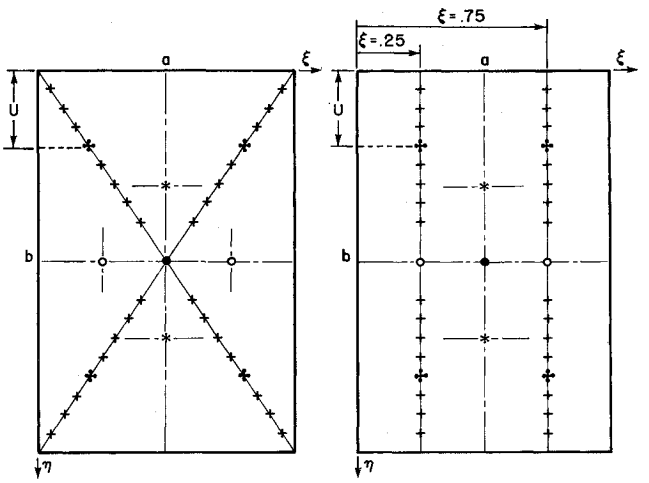

Fig. 2 Distribution of rigid point support locations and attached masses: a) plate A; b) plate B (typical four point clusters required to simulate rigid point support are shown at distances U from plate edges).

two equal masses were located on the plate short central axis, each 2.5 in. (63.5 mm) from the center. In the final configuration, the same pair of masses was located on the plate long central axis, each at a distance of 3.0 in. (76.2 mm) from the center. The nominal weights of the attached masses varied from 50 to 300 g in 50-g intervals. The nominal weight of the test plates was 404 g. Inevitably, weights varied slightly from these nominal values; however, exact weights were used in all computations. The objective of the experimental study was to establish resonant frequencies and the associated mode shapes for the two sets of plates A and B. For this purpose, the method of impact testing[2] was adopted.

B. Comparison of Experimental and Computed Frequencies

Measured and computed fundamental mode frequencies for the entire array of rigid support point and attached mass configurations were compared. It was found that in the vast majority of cases agreement was within about 3%. One of these comparisons is presented in Table 1. One may observe a slight difference between experimental frequencies reported here for the case of zero attached mass and results reported earlier in Ref. 2. Such small differences result from the use of a slightly different plate mounting rig. Additionally, a comparison of

the computed and the experimentally measured mode shapes was made for all of the frequencies and good agreement was obtained.

IV. Discussion and Conclusions

It is concluded that the theoretical model as described herein predicts frequencies and mode shapes that are in good agreement with experiment.

It has been observed that accurate prediction of higher mode frequencies, for plates of the type discussed here, often requires inclusion of the effects of rotary inertia of attached masses in the analysis. This is not surprising as the masses will undergo harmonic rotation for some of the higher modes. Extension of the analysis to include these rotary inertia effects is currently underway.

To the authors' knowledge, the work reported here represents the first comprehensive analytical and experimental study of this interesting and timely problem. The analysis provides the designer with a powerful tool for optimizing the distribution of rigid point supports and attached masses on the plate surface. The experimental data will provide other researchers with reference points against which they can compare their theoretical results.

Acknowledgments

This work was supported by a grant from the National Sciences and Engineering Research Council of Canada. Experimental work was carried out at the David Florida Laboratory of the Canadian Space Agency in Ottawa, Canada.

References

[1]Gorman, D. J., "A Note on the Free Vibration of Rectangular Plates Resting on Symmetrically Distributed Point Supports," *Journal of Sound and Vibration,* Vol. 131, No. 3, 1989, pp. 515-519.

[2]Gorman, D. J., and Singal, R. K., "Analytical and Experimental Study of Vibrating Rectangular Plates on Rigid Point Supports," *AIAA Journal,* Vol. 29, No. 5, 1991, pp. 838-844.

Objective Functions for the Nonlinear Curve Fit of Frequency Response Functions

José Roberto F. Arruda
State University of Campinas, 13081 Campinas, São Paulo, Brazil

Introduction

THE improvement of finite element models of structures based on experimental data is usually referred to as model updating. Finite element model updating methods in structural dynamic problems generally consist of making corrections of the theoretical stiffness and mass matrices so that the eigenvalues and eigenvectors of the finite element model get closer to the experimental values.[1] The number of parameters in the finite element model is normally too big, and constraint equations[2] or localization methods[3] must be used to reduce the number of parameters of the theoretical model that must be estimated. The parameter estimation method may be interpreted as an optimization method where the minimization of an objective function is sought. Depending on how this function is constructed, the estimation method may be classified as least squares (LS), maximum likelihood (ML), or maximum a posteriori (MAP),[8] which can be either linear or nonlinear and recursive or not. In finite element model updating problems, it is frequent that for the most part the structure be well modeled, whereas localized regions are very poorly modeled, e.g., mechanical joints.[4,5] In such cases, there is generally very little confidence in the initial guess parameter values of the theoretical model and LS or ML estimation methods are suitable. In previous publications, the author has proposed the nonlinear curve fit of dynamic response functions, e.g., frequency response functions (FRF) and unbalanced responses, for such applications.[6,7] It was observed in the various examples treated in those papers that taking the response curves in logarithmic scale improved the convergence of the search procedures involved in the minimization of the objective function. In this paper, it is shown that the minimization of the correlation coefficient between two curves may be obtained in an iterative process where each step consists of a least squares nonlinear fit with a scaled curve. It is also shown that, when the curve is in logarithmic scale, the least squares objective function has the same shape as the maximum correlation objective function, and they are related by a scalar that is the square of the norm of the fitted data vector.

Objective Functions

If F_x is a vector that contains the experimental values of a response function, e.g., a FRF, and F_t is the corresponding vector of theoretically predicted values for the same function, the ordinary least squares objective function J_{LS} is given by,

$$J_{LS}(p) = (F_x - F_t)^T(F_x - F_t) \tag{1}$$

where p is a vector of which the elements are the parameters used in the theoretical model to calculate F_t, and superscript T denotes the transpose of a vector. The objective function for maximizing the correlation coefficient between the two curves may be written as,

$$J_{MC}(p) = 1 - \frac{(F_x^T F_t)^2}{(F_x^T F_x)(F_t^T F_t)} \tag{2}$$

Figures 1 show both objective functions in the case of a one degree-of-freedom (DOF) structure where the absolute value of the FRF was taken as the response function to be fitted.

$$|H(k,m,c,\omega)| = \left|\frac{1}{k - m\omega^2 + i\omega c}\right| \tag{3}$$

In Eq. (3), k is the stiffness coefficient, m the mass, c the damping coefficient of the one-DOF structure, and ω the frequency in radians per second. The curves shown in Figs. 1 are cross sections of the objective functions $J_{LS}(p)$ and $J_{MC}(p)$ in the neighborhood of the solution $p_0 = \{k_0, m_0, c_0\}^T$. The LIN and LOG superscripts are used when the absolute value of the FRF or its logarithm are used, respectively. The curves were scaled for plotting so that the amplitudes would be smaller than 1. It can be seen in Figs. 1 that when the logarithm of the FRF is used the objective functions have the same shape for LS and MC and that this shape is much smoother than for LS with linear FRF amplitudes. The sawtooth profile of the cross sections of $J_{LS}^{LIN}(p)$ explains the poor convergence of the nonlinear search process when the initial guess values of p are not in a close neighborhood of the solution p_0.

Nonlinear Search Algorithm

The Gauss-Newton solution for the minimization of $J_{LS}(p)$ gives the well-known nonlinear LS iterative search algorithm:

$$p^{k+1} = p^k + (S^T S)^{-1} S^T (F_x - F_t) \tag{4}$$

where k denotes the iterative step and S is the sensitivity matrix given by the Jacobian of function F_t with respect to the

Received Feb. 6, 1991; revision received May 21, 1991; accepted for publication May 29, 1991.

*Associate Professor, Department of Computational Mechanics.